Taylor-Caulfield Instabilities in a Layered Stratified Shear Flow

Giordano Ponetti and Neil J. Balmforth

Dipartimento di Matematica e Informatica,
Università di Palermo, Italy
giordano.ponetti@dmi.unict.it
Department of Mathematics,
University of British Columbia, Canada
njb@math.ubc.ca

Abstract

We study the stability of interfacial waves in a stratified shear flow where the density profile takes the form of a staircase of interfaces separating uniform layers, such as may arise from double-diffusive processes in lakes and oceans. Internal gravity waves riding on density interfaces can resonantly interact due to a background shear flow, resulting in the Taylor-Caulfield instability. The many steps of the density profile permit a multitude of interactions between different interfaces, and a rich variety of Taylor-Caulfield instabilities.

We provide a linear instability analysis for a staircase with piecewise-constant density profile, allowing for an arbitrary number of interfaces. The staircase is embedded in a background linear shear flow. For long wavelength, weakly nonlinear structures in weakly stratified fluid, we study the onset of instability. Fully nonlinear states are studied numerically in the long-wave and weak stratification limit.

1 Introduction

We explore the Taylor-Caulfield instabilities (TCI) that may arise in a stratified fluid with a staircase density profile and background shear flow. The classical Kelvin-Helmholtz instability is the most well-known variety of stratified shear instability and is commonly interpreted at the resonant interaction of waves riding on vorticity interfaces. Holmboe waves (HWI) are the next most studied type of instability, arising when a wave on a vorticity interface resonantly interacts with a gravity wave lying at a density interface Holmboe (1962). KHI and HWI are considered robust instabilities in the sense that they have been observed in natural systems and experiments.

Taylor (1931) also pointed out the possibility of a third instability in which waves riding on density interfaces could resonantly interact when their phase speeds become locked due to the Doppler-shifting effect of a background shear flow. This instability has been more elusive to observe, with the scientific community more concerned with why one might find basic states with layered density profiles in the first place. Taylor's instability was quantified and studied in more detail by Caulfield (1994), in parallel with some first laboratory experiments Caulfield et al. (1995) and nonlinear simulations Lee and Caulfield (2001). Balmforth et al. (2012) provided a comprehensive study of TCI in the long-wave limit that two density interfaces were considered as a stratified "defect" in the shear flow.

Here we explore the linear stability and nonlinear evolution of multiple TCI growing on layered density profiles. We consider a density staircase with equally spaced steps of equal size superposed on a background linear shear flow. We study normal mode solutions of the incompressible 2D Navier-Stokes and heat equations under the Boussinesq approximation. Our results show a predominance of near-neighbor interfaces TCI which are particularly strong in the limit of small bulk Richardson numbers and wavenumbers. This limit allows

to consider the defect theory approximation Balmforth et al. (2012) where by a multiple scale expansion it is possible to reduce the governing equations to a Vlasov-like problem. This limit allow us to study the nonlinear evolution of internal gravity waves of large wavelength and their mixing effect.

2 Formulation

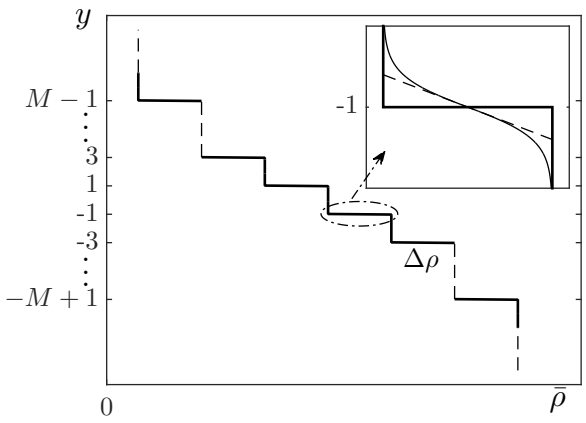

Figure 1: Background staircase density profile for $M+1$ equally spaced layers of equal size. The steps are separated by a dimensionless distance of 2 and symmetrically placed about $y=0$; the density jump across each interface is $\Delta\rho$. The inset shows the three types of interface profile that we use throughout the paper, as given in (4): the thick line is a piecewise-constant interface; the dashed line represent a piecewise-linear interface; and the thin line is the hyperbolic tangent interface.

We consider a two-dimensional viscous and diffusive stratified fluid in the Boussinesq approximation: using a vorticity-buoyancy-streamfunction formulation these are

$$\zeta_t + \psi_x\zeta_y - \psi_y\zeta_x + y\zeta_x = b_x + \nu\big(\zeta_{xx} + \zeta_{yy}\big), \tag{1}$$

$$b_t + \psi_x b_y - \psi_y b_x + y b_x + B_y\psi_x = \kappa\big(b_{xx} + b_{yy}\big), \tag{2}$$

where t is the time and (x,y) is the coordinate system where y points upward. The non-dimensional parameters are the inverse Reynolds number ν and the inverse Péclet number κ. The streamfunction $\psi(x,y,t)$, vorticity $\zeta(x,y,t)$ and buoyancy $b(x,y,t)$ that appear in the equations represent perturbations away from a background state characterized by a horizontal velocity profile $U(y)=y$ and buoyancy profile $B(y)$ The domain is infinitely deep and periodic in the horizontal direction: $(x,y)=[0,2\pi]\times[-\infty,\infty]$. We assume the three scalar fields to decay exponentially as $y\to\pm\infty$. The multiple layer background buoyancy field is

$$B_y(y) = J\sum_{j=0}^{M/2-1}\Big[\Theta(y-2j-1)+\Theta(y+2j+1)\Big], \tag{3}$$

where J is the bulk Richardson number, M is the number of interfaces and $\Theta(y)$ is an interface function that prescribes the shape of the steps of the staircase (see figure 1): we use the piece-wise constant, linear or smooth profiles,

$$\Theta(y) = \begin{cases} \delta(y) \\ [1-\mathrm{sgn}(|y|/d-1)]/(4d) \\ (2d)^{-1}\mathrm{sech}^2(y/d) \end{cases}, \tag{4}$$

where d is the characteristic thickness of the interface, when finite.

When the vertical extent of the staircase is relatively small compared to the horizontal domain, matched asymptotic expansion can be used to reduce equations (1) and (2) to the Vlasov-like problem,

$$\mathscr{Z}_t + \eta \mathscr{Z}_x + \Phi_x \mathscr{Z}_\eta + \Phi_x B_{\eta\eta} - \nu \mathscr{Z}_{\eta\eta} = 0, \tag{5}$$

$$\mathscr{L}\Phi = \int_{-\infty}^{+\infty} \mathscr{Z}\, d\eta - \langle \mathscr{Z} \rangle = -2 \sum_{n=-\infty}^{\infty} |n| \Phi_n(t) e^{inx}, \tag{6}$$

Here, $\mathscr{Z}(x,\eta,t) = \zeta + b_\eta$ and $\Phi(x,t)$ is the leading-order streamfunction over the "stratified defect", which is resolved using the rescaled coordinate $\eta = y/\epsilon$, where ϵ is the ratio of the vertical and horizontal lengthscales. We have also assumed that $\kappa = \nu$ and introduced a suitable rescaling of time (see Balmforth et al. (2012)).

3 Discussion

As shown in previous work (Sutherland (2010) and Carpenter et al. (2011)), TCI can be interpreted as a resonance between gravity waves supported by different density interfaces that arises when the Doppler-shifting effect of the background flow allows their horizontal phase speeds to lock together. This resonance requires a suitable choice for the bulk Richardson which controls the natural phase speed of the waves in the absence of flow. For M interfaces, there are $\binom{M}{2}$ possible resonances that may lead to TCI when J is properly tuned. To search for these resonances, we linearize equations (1) and (2) and look for normal mode perturbations of the form,

$$[\psi, \zeta, b](x,y,t) = [\widehat{\psi}, \widehat{\zeta}, \widehat{b}](y) \exp[ik(x-ct)] \tag{7}$$

where k is wavenumber and c phase speed. This reduces the nonlinear problem to the Taylor-Goldstein equation,

$$\left(\frac{d^2}{dy^2} - k^2 \right) \widehat{\psi} = -\frac{B_y}{(y-c)^2} \widehat{\psi}, \tag{8}$$

which can be turned into an integral equation using the Green function of the operator on the left-hand side:

$$\widehat{\psi}(y) = \frac{1}{2k} \int_{-\infty}^{+\infty} \frac{B_y(\xi)\widehat{\psi}(\xi)}{(\xi-c)^2} e^{-k|y-\xi|} d\xi. \tag{9}$$

For the discontinuous interface profile in (4), this integral equation can be immediately turned into a matrix eigenvalue problem for c, with eigenvector

$$\mathbf{X} = \left(\Psi_{M-1}\, \Psi_{M-3}\, \ldots\, \Psi_1\, \Psi_{-1}\, \ldots\, \Psi_{-M+3}\, \Psi_{-M+1} \right)^T, \qquad \Psi_{\{y\}} = \frac{\widehat{\psi}(y)}{(y-c)^2}.$$

If we denote the matrix of coefficients of the Ψ_j's by $\mathscr{G}_M$, the dispersion relation is given by $D_M(c,J,k) = \det(\mathscr{G}_M) = 0$, which is a polynomial of order $2M$ in c.

In the limit of large wave numbers the off-diagonal elements of $\mathscr{G}_M$ are negligible, which means that the vorticity of internal gravity waves fades quickly away from any interface

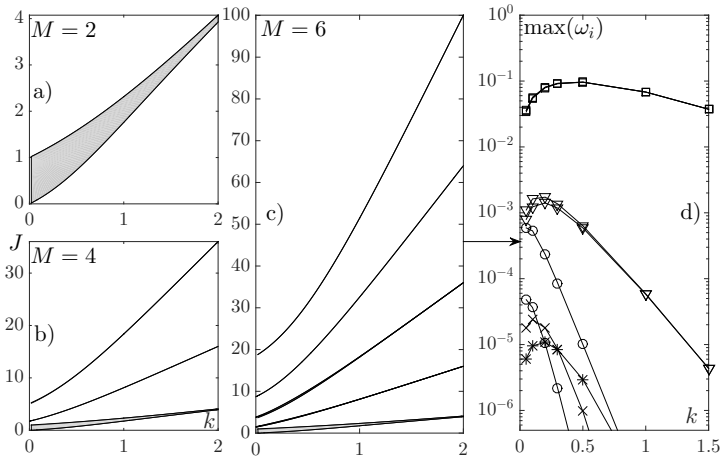

Figure 2: Stability boundaries and growth rates for M =2, 4 and 6 piecewise-constant interfaces. The solid lines are the marginal stability boundaries for TCI and the gray shaded regions are where the unstable modes lies. The right panel shows the maximum growth rate over each band in J of unstable waves when $M = 6$. Growth rates are labelled as follows: ($\square$) are near-neighbor, ($\bigcirc$) are next-neighbor, ($\bigtriangledown$) are third-neighbor, ($\times$) are fourth-neighbor and ($*$) are fifth-neighbor resonances.

and thus the waves weakly overlap. This reduces the matrix problem to a product of the diagonal terms,

$$\prod_{j=-M/2}^{M/2-1} \left[\frac{2k}{J} \Big(2j + 1 - c \Big)^2 - 1 \right] = 0, \tag{10}$$

which implies phase velocities $c_r = 2j + 1 \pm \sqrt{J/2k}$. We now look for waves with equal phase speed after being doppler shifted in opposite directions: when $J = 2k$ we find the first phase-locking which occurs for nearest-neighbor interfaces; the associated phase speeds are $c_r = 0, \pm 2, \pm 4, \ldots, \pm(M-2)$. A bigger J unlocks the next-nearest-neighbor resonances when $J = 8k$ giving $c_r = \pm 1, \pm 3, \ldots, \pm(M-3)$. Third-nearest-neighbor resonances are activated when $J = 18k$, where waves drifting at $c_r = 0, \pm 2, \pm 4, \ldots, \pm(M-4)$ become unstable. The repeating structure of the resonances is now evidenced and indicates how to relate the Richardson number to the "order" r of the interaction, defined such that $r = 1$ signifies nearest-neighbor interactions, next-nearest-neighbor interactions have $r = 2$, and so on. Evidently, $J = 2r^2 k$, which provides the $k \gg 1$ asymptotes of the instability bands.

For lower wavenumber, the vertical decay of the internal gravity waves is slower and the off-diagonal elements of $\mathscr{G}_M$ become important. The instability bands open up as shown in figure 2 to reveal their full structure on the (k, J)-plane. Clearly, the larger the number of density interfaces, the more resonances are possible and the more instability bands form. In panel d) of figure 2 we plot the maximum growth rate over J for each of the bands. The nearest-neighbor resonances are the strongest instabilities, while further-neighbor resonances are thinner and orders of magnitudes weaker, which probably makes them difficult to be observed.

Instability is therefore most likely due to near-neighbor interfaces. Before exploring their nonlinear development, we focus briefly on the effect of a finite interface thickness on the linear stability. We consider two interfaces with the piecewise-linear profile in (4).

The solution of (8) is now

$$\psi = \begin{cases} A_+ e^{-k(y-1)} & y > 1+d \\ \psi_+ & |y-1| < d \\ B_+ e^{ky} + B_- e^{-ky} & |y| < 1-d \\ \psi_- & |y+1| < d \\ A_- e^{+k(y+1)} & y < -1-d. \end{cases} \tag{11}$$

By imposing the continuity of the streamfunction and its derivative, we then arrive at the dispersion relation $D_d(c,k,J)=0$ that predicts the results in in figure 3. The instability

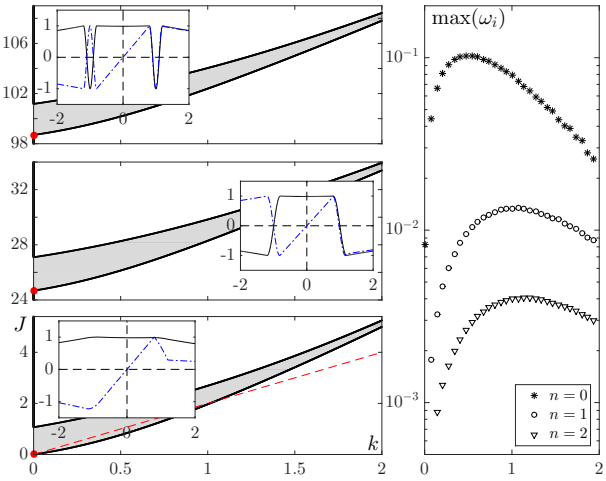

Figure 3: Instability bands and growth rates for waves riding on two piecewise-linear interfaces of thickness $d=0.2$. In the left panels we show the instability bands as shaded regions. The red dots mark $J=(n\pi)^2/2d$ and the red dashed line is the $k \gg 1$ limit, $J=2k$, for discontinuous interfaces. In the insets we show the solutions for ϕ on the upper ($.-$) and lower ($-$) marginal stability boundaries for $k=0.2$. In the right panel we show the maximum growth rate inside the first five instability bands.

band with the lowest J follows the result for a discontinuous pair of interfaces for small k. However, the band then bends upward away and from the asymptote $J=2k$. More instability bands are also available at specific Richardson numbers, which correspond to normal modes with an increasing number of spatial oscillations within each interface. Using perturbation methods it is possible to find the critical Richardson number for the lower marginal stable boundary of each band: $J=(n\pi)^2/2d$, as marked in figure 3. As for the piecewise-constant stratified fluid, we observe weaker growth in the higher Richardson number bands.

As we already mentioned the strongest instabilities grow between near-neighbor interfaces and their instability bands are stacked altogether in the same region of the (k,J)-plane. The defect approximation presented in Balmforth et al. (2012) can be used to analyse these resonances and study their nonlinear dynamics when J and k are small. Looking for normal-mode solutions to (5) and (6), we find the dispersion relation

$$\frac{k}{J} = \sum_{j=0}^{M/2-1} \frac{(2j+1)^2 + c^2}{[(2j+1)^2 - c^2]^2}, \tag{12}$$

when the background density distribution is piecewise-constant. Sample solutions for $c_i = \mathrm{Im}(c)$ as a function of J/k are shown in figure 4 for $M=2$ and 4.

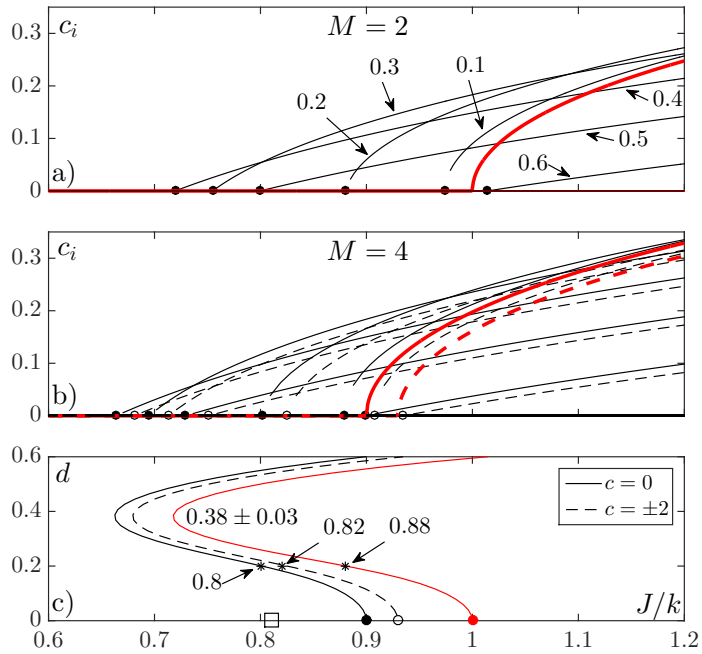

Figure 4: $c_i = \omega/k$ against J/k for different interfaces thicknesses d, for (a) $M = 2$ and (b) $M = 4$. The solid lines refer to modes with $c_r = 0$ and the dashed lines to $c_r = \pm 2$. The thicker red lines show the results for the piecewise-constant profile. The filled and open circles indicate the critical values, $\bar{J}(0, d)$ and $\bar{J}(2, d)$, respectively. In panel c) we show these two functions for $M = 4$ (black solid and dashed lines) and $M = 2$ (red line).

In our numerical simulations we consider finite thickness interfaces. The effect on the critical Richardson numbers and growth rates of smoothing out the interface using the smooth profile in (4) is shown in figure 4. The effect is non-monotonic, with the smoothing first lowering the critical value of J/k, but then increasing it, and largely suppressing the growth rate. For our numerical simulations we pick $d = 0.2$ to lower the computational cost of simulating sharp interfaces whilst allowing for relatively fast growing perturbations.

The nonlinear evolution of TCI in a three layer fluid has been studied in Balmforth et al. (2012) using the defect approximation. Here we add two more layers ($M = 4$) allowing for more potential resonances. However, the defect approximation only captures the nearest-neighbor interaction. We set $\nu = 10^{-6}$ and consider smooth interfaces of thickness $d = 0.2$.

For two layers, TCI causes the density interfaces to deform and approach one another. The interfaces then connect and generate an elliptical billow which is embedded by vorticity filaments. The billow moves at the phase-lock velocity and pulses slightly in time. In our simulations with $M = 4$, we find that the three possible nearest-neighbor resonances can generate unstable modes that lead to the growth of billows centered at $y = -2$, 0 and 2, each traveling at the local flow speed. Which of the three cases is first seen depends on whether the corresponding linear mode is unstable and on the fashion in which the system is kicked into action: we initialize our initial-value problems by adding onto the basic state one of the linear modes with a given amplitude, setting J such that the mode is either linearly stable or unstable. Which billow is seen depends on which mode is used for the initialization and how strongly it is forced.

In the linearly unstable regime, the initial kick to a particular mode seeds the growth of that TCI, which subsequently grows to finite amplitude where nonlinear effects arrest its growth in the formation of a billow structure. Individually each of the three types of

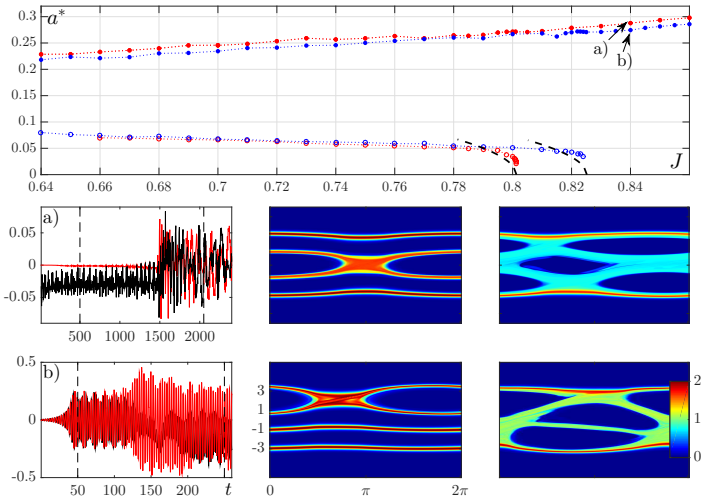

Figure 5: Bifurcation diagram of the saturation amplitude a^* agains the Richardson number J. We consider $M = 4$, $d = 0.2$, $\nu = 10^{-6}$ and focus on pure modes with $k = 1$ and phase velocity $c = 0$ or ± 2. The two thick dashed curves are the predicted amplitudes of the weakly nonlinear analysis. In panels a) and b) we report solutions for $J = 0.84$ where the left panels show the real ($-$) and imaginary ($-$) part of mode $\Phi_1(t)$ and the vertical dashed lines mark the snapshots on the right.

billows looks much like that seen for two interfaces, though the billows now also mildly perturb the other interfaces that do not participate in the resonant interaction. Moreover, although each can survive for sustained periods, single billows do not persist indefinitely; eventually the perturbations to the other interfaces trigger the growth of the other resonant modes to lead to nonlinear states with multiple billows; see figure 5. This occurs whether the other modes are linearly unstable or not. Indeed, we can trigger the formation of a particular billow by forcing the corresponding mode sufficiently strongly even when it is linearly stable, in the manner of a subcritical transition.

To track the onset of nonlinear states we measure the amplitude at which the linear instability first appears to saturate a^* (the first maximum of the L_2-norm of Φ); see figure 5. In Balmforth et al. (2012) this parameter was exploited to detect a subcritical bifurcation for sufficiently sharp interfaces. The same scenario emerges here, with each of the TCI modes leading to nonlinear states below the onset of linear instability. As in Balmforth et al. (2012), the bifurcating branches of nonlinear solutions are consistent with a weakly nonlinear analysis for interfaces of zero thickness.

Moving to higher Richardson numbers allow TCI modes with smaller horizontal wavelength to become unstable. These generate multiple billows arrayed horizontally. However, these states suffer a secondary instability in which the horizontally aligned billows merge with one another to lead to a single large-scale billow per layer. As seen in figure 6 the secondary instability takes the form of a vortex pairing instability.

4 Conclusions

Multiple Taylor-Caulfield instabilities can arise in stratified shear flows with a staircase density profile. The more steps in the staircase, the more potential modes of instability. Of these, the resonant interactions between neighboring density interfaces are responsible for the strongest instabilities. We have taken advantage of the occurrence of these modes at low wavenumber and bulk Richardson number to exploit the defect approximation of Balmforth et al. (2012) and simply the analysis of these instabilities. We have observed

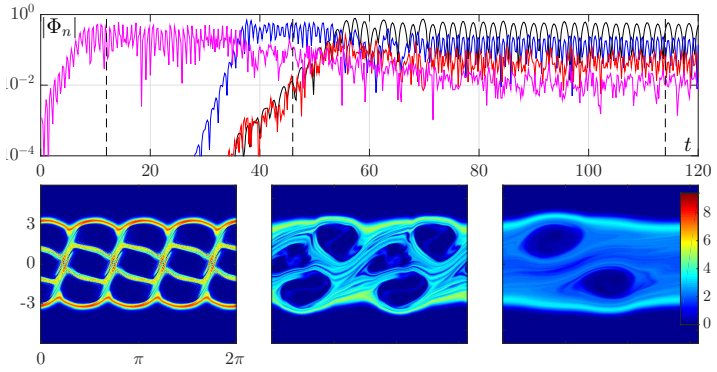

Figure 6: Billows merging for an initial perturbation with $k = 4$. We consider $M = 4$, $d = 0.2$, $\nu = 3{\cdot}10^{-4}$ and $J = 3.6$ which allow wavenumbers $k = 1$, 2, 3 and 4 to be unstable. We show the time evolution of $|\Phi_n|$ where the black, blue, red and magenta lines are for $k = 1$, 2, 3 and 4 respectively. The three solution snapshots show the merging of billows and are marked by vertical dashed lines in the top panel

that TCI can lead to the formation of billows inside any of the density layers. Forcing with a single TCI leads to its linear growth and the formation of a single billow, but eventually all the other modes are triggered to lead to a multiple billow state. Vertically arrayed billows coexist, but vortex-pairing instabilities appear to always cause horizontally aligned billows to merge.

References

Balmforth, N. J., Roy, A., and Caulfield, C. P. (2012). Dynamics of vorticity defects in stratified shear flow. *Journal of Fluid Mechanics*, 694:292–331.

Carpenter, J. R., Tedford, E. W., Heifetz, E., and Lawrence, G. A. (2011). Instability in stratified shear flow: Review of a physical interpretation based on interacting waves. *Applied Mechanics Reviews*, 64(6):060801.

Caulfield, C. P. (1994). Multiple linear instability of layered stratified shear flow. *Journal of Fluid Mechanics*, 258:255–285.

Caulfield, C. P., Peltier, W. R., Yoshida, S., and Ohtani, M. (1995). An experimental investigation of the instability of a shear flow with multilayered density stratification. *Physics of Fluids*, 7(12):3028–3041.

Holmboe, J. (1962). On the behavior of symmetric waves in stratified shear layers. *Geophys. Publ*, 24:67–113.

Lee, V. and Caulfield, C. P. (2001). Nonlinear evolution of a layered stratified shear flow. *Dynamics of atmospheres and oceans*, 34(2):103–124.

Sutherland, B. R. (2010). *Internal gravity waves*. Cambridge University Press.

Taylor, G. I. (1931). Effect of variation in density on the stability of superposed streams of fluid. *Proc.R.Soc.London*, 132:499–523.